

# Compressibility Behaviour of Warp Knitted Spacer Fabrics Based on Elastic Curved Bar Theory

Fatemeh Mokhtari, Mahnaz Shamsirsaz, Masoud Latifi, Mohammad Maroufi

Amirkabir University of Technology, Tehran, IRAN

Correspondence to:

Mahnaz Shamsirsaz email: [shamshir@aut.ac.ir](mailto:shamshir@aut.ac.ir)

## ABSTRACT

Nowadays, the mechanical characterization of 3-D spacer fabrics has attracted the interest of many textile researchers. These Spacer fabrics present special mechanical and physical characteristics compared to conventional textiles due to their wonderful porous 3-D structures. These fabrics, produced by warp knitting method, have extensive application in automobile, locomotive, aerospace, building and other industries. In these applications, the compressibility behaviour plays a significant role in the fabric structural stability. This compressibility behaviour could be affected by different knitting parameters such as density of pile yarn, fabric thickness, texture design etc.

The aim of this paper is to introduce and develop an appropriate elastic theoretical model to predict the compressibility behaviour of warp knitted spacer fabric (WKSF). Three theoretical models are proposed, based on modelling pile yarns as the curved bars and are improved in three steps: a) with same curvatures in weft and warp directions (model A), b) curved bar for warp direction and cantilever bar for weft direction (model B), and c) curved bars with two different curvatures in weft and warp directions considering the curvature variations under loading (model C: improved model). The results obtained by the proposed models have been compared with previous model based on simply cantilever bars theory in literature. The results show that the simulation data obtained by the model C are closer to the experimental results comparing to the models A and B. Model C based on different weave parameters could better predict the elastic compressibility behaviour of this kind of WKSF in order to compare with previous models.

**KEYWORDS:** Spacer fabrics, Compressibility behaviour, Theoretical modelling, Elastic curved bar theory, Weft and warp curvatures variations under loading

## INTRODUCTION

Spacer knits are double-layered circular knits with a cushion of air and “spring-like” yarns between the two sides. This unique fabric class is knit in one continuous operation. Although it looks like several fabrics bonded together, it is actually one fabric which cannot be separated by layer. Special yarns are selected for aesthetic qualities (i.e.: soft hand, bright/dull, etc.) and for performance properties (i.e.: moisture transport, thermal insulation or conductance, anti-microbial, compressibility etc.). Compressibility is known as an important mechanical property of textiles. In Murthyguru theory, compressibility can be defined as a decrease of initial thickness due to appropriate increase of compressive force at measuring time [1]. In this definition, initial thickness of tissue is considered as thickness without applied force.

The most important and fundamental theory related to the compressibility of textiles is Van Wyk theory. In his theory, he introduced a relationship between volume and stress for raw wool fibers regardless of their friction, twist and strength of fibres during compressibility [2]. However, few works have been done on modelling of compression behaviour of warp knitted spacer Fabrics [3,4,5].

Hong and Ming obtained the stress-strain curve of warp knitted spacer fabrics (WKSF) experimentally, and calculated the contact pressure of WKSF assuming this pressure is exerted in two different ways: by solid plate and ball indentation [3]. Their objective was finding the relationship between the construction parameters and indentation hardness. They reported that more efforts should be done to calculate the deformations in order to analyze the compressibility behaviour of WKSF (stress-strain curve).

Numerical modelling of the compression behaviour of WKSF was carried out using Finite Element Analysis (FEA) based on bar, solid and shell theory [4]. The principle of the proposed methodology was the replacement of the discrete structure of each layer by a continuum structure presenting an identical mechanical performance.

The mechanical characteristics and the damage modes of these mono-spacer fabric composites under different load conditions have been explored experimentally by Min Li et al. [5]. Also, they analysed the effects of pile height, pile distribution density and pile structure on the composites mechanical performances using the experimental results.

Compressibility of the spacer fabrics depends on the type of spacer yarn, the yarn count of the spacer yarn, the stitch density and the spacer yarn configuration [6]. In different applications, compressibility can be adjusted by appropriate selection of these parameters [5]. Musial introduced a cantilever bar theory of transverse deformation in textile products consisting of two external layers combined with deformed elements in the middle layer [7]. Hong and Ming presented the compressibility of WKSF based on its construction and analyses the stress and strain behaviour of spacer fabric when compressed [3].

The aim of this research is to predict elastic compressibility behaviour of WKSF using three different configurations as curved and cantilever bars for monofilaments; model A) with same constant curvatures in weft and warp directions model B) constant curved bar for warp direction and cantilever bar for weft direction and model C) curved bars with two different curvatures in weft and warp directions, considering the variation of curvature radius and angle with compression loading. These three models are based on spring constants parameters in elastic curved and cantilever bar theory. The results show that the simulation data obtained by model C are closer to the experimental results of these spacer fabrics comparing to the other theoretical models.

### THEORETICAL MODELS

Three different theoretical models: named here models A, B and C for spacer fabric have been proposed and developed. In model A, the monofilament compression deflection has been modelled as the deflection of the curved bars with same curvature in weft and warp directions. In model B, monofilaments in weft and warp directions are

considered as cantilever bar and curved bar respectively. Finally, in model C, the monofilaments are modelled with two different curvatures in weft and warp directions as the curved bars. Also, the variations of curvature radius and angle in weft and warp directions during compression loading increase have been considered in model C. Since these three models are based on classical elastic curved bar theory in compression, this will be described first in the following section.

### CURVED BAR THEORY

This theory is based on the small deformations of an elastic coplanar curved bar presented in the literature [8]. Each point on the cross section of this bar is displaced from its unstrained position through small components  $u$ ,  $v$  and  $w$  along  $x$ ,  $y$  and  $z$  directions respectively *Figure 1*.  $u$ ,  $v$  and  $w$  are the continuous single-value functions of the coordinates and, in the case of a curved bar,  $u$  and  $v$  represent tangential and radial deflections of points on the cross section and  $w$  represent the deflection in a direction normal to the plan of the bar (the  $z$  direction). It is assumed that the cross section of the bar remains plane after deformation and also the bar material is linearly elastic, homogeneous, isotropic, and continuous. This allows to take advantage of the principle of superposition and to study each of these deflection components separately.

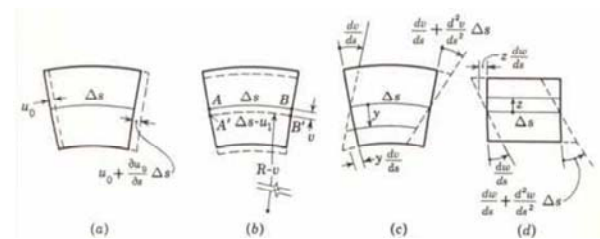


FIGURE 1. Deformation of a curved bar element [8]

The radius of curvature of the bar has been denoted as  $R$ . An orthogonal coordinate ( $x, y, z$ ) is assigned on the cross section of the bar. The  $x$  axis is along to longitudinal direction of the bar, the  $y$  is the radial coordinate which directing toward the centre of curvature and  $z$  is perpendicular to the plan of the bar. It is assumed that the bar deflects in  $x$ - $y$  plan and the deflection in the  $z$  direction has been neglected.

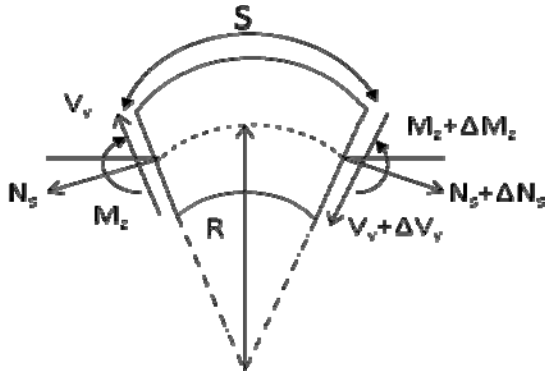


FIGURE 2. An element along the curved bar

Considering *Figure 2*, the equilibrium equations can be written in the cantilever and horizontal directions as:

$$\frac{dV_y}{ds} = -\frac{N_s}{R} \quad (1)$$

$$\frac{dN_s}{ds} = \frac{V_y}{R} \quad (2)$$

The Equilibrium condition around z axis rotation results in:

$$\frac{dM_z}{ds} = V_y \quad (3)$$

Finally by twice differentiation of Eq. (3) and using the Eq. (1) and Eq. (2), Eq. (4) which is the equilibrium equation in the term of moment, can be obtained [8].

$$\frac{d^2 M_z}{ds^2} + \frac{1}{R^2} \frac{dM_z}{ds} = 0 \quad (4)$$

Due to circular shape of the monofilaments, the radius of the curvature is assumed to be constant along bar length.  $\frac{dR}{ds} = 0$  is considered.

To obtain the relationship between  $M_z$  and deflections components of the bars cross section, the deflections of the bar has been defined. The absolute deflection of a point is obviously the vector sum of the three independent components. In fact, the complete deformation of a bar element can be considered to be due to three different

deflections:  $u_0$ , a deflection of points on the cross section due to a stretching of the central axis;  $u_1$ , a shortening of the fibres due to a decrease in the radius of curvature  $R$  by an amount  $v$ . These deflections are illustrated in *Figure 1*.

To obtain bending moment in bar, the stress in the cross section must be obtained. The stress can be calculated by cross section deflections. After some mathematical manipulations, the Eq. (5) for bending moment is obtained [8].

$$M_z = -E \left[ J_z \left( \frac{d^2 v}{ds^2} + \frac{v}{R^2} \right) \right] \quad (5)$$

It is emphasized  $v$  is the deflection in the radial direction and deflection along Z axis has been neglected. In above equation  $J_z$  is defined as:

$$J_z = \int \frac{y^2}{1 - \frac{y}{R}} dA \quad (6)$$

In the specific case of monofilaments because their radius curvature are very large in compare with their cross section radius the  $\frac{y}{R}$  ratio is negligible and  $J_z$  can be calculated as:

$$J_z = \int y^2 dA = I_z \quad (7)$$

Finally, according to Eq. (4) and Eq. (5), the alternative form of the differential equation for the elastic curve has been obtained.

$$EI_z \left( \frac{d^5 v}{ds^5} + \frac{2}{R^2} \frac{d^2 v}{ds^2} + \frac{1}{R^4} \frac{dv}{ds} \right) = 0 \quad (8)$$

The general solution of (8) is given as:

$$v = c_1 \cos \phi + c_2 \sin \phi + c_3 \phi \cos \phi + c_4 \phi \sin \phi + c_5 \quad (9)$$

As it is obvious in Eq. (9), to obtain the unique solutions, 5 boundary conditions are required to determine the five unknown coefficients ( $c_i (i=1 \text{ to } 5)$ ). Considering *Figure 3* the boundary conditions are described.

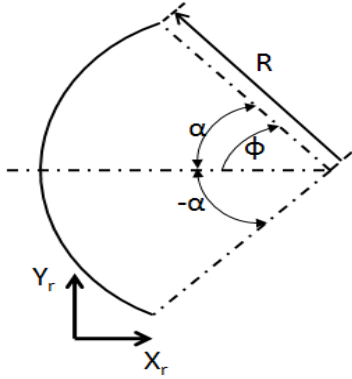


FIGURE 3. Schematic of a monofilament which is considered as curved bar

By assuming that monofilaments don't move in radial direction, the first boundary condition in  $\varphi = -\alpha$  is proposed as:

$$v|_{\varphi=-\alpha} = 0 \quad (10)$$

Considering that the surface layer above and below the monofilaments cannot exert moments on the monofilaments, two boundary conditions are presented in Eq. (11) and Eq. (12).

$$M_z|_{\varphi=\alpha} = 0 \quad (11)$$

$$M_z|_{\varphi=-\alpha} = 0 \quad (12)$$

By taking into account the bending moment definition in Eq. (5), Eq. (11) and Eq. (12) can be written as Eq. (13) and Eq. (14) respectively.

$$\frac{d^2v}{d\varphi^2} + v|_{\varphi=\alpha} = 0 \quad (13)$$

$$\frac{d^2v}{d\varphi^2} + v|_{\varphi=-\alpha} = 0 \quad (14)$$

During compressibility testing procedure, a total force is applied on the whole surface of the sample. To calculate the force for each monofilament, total force must be divided by the number of the monofilaments in the sample area. The equilibrium equation on the cross section of the monofilament due to equivalent force is:

$$F = N_s \cos \alpha - V_y \sin \alpha \quad (15)$$

Where  $F$  is to equivalent force which is applied to each monofilaments. In the above equation, the shear force can be obtained by Eq. (3). By replacing  $ds$  in Eq. (4) with  $ds = R d\varphi$ , Eq. (16) can be achieved as follow:

$$V_y = \frac{1}{R} \frac{dM}{d\varphi} \quad (16)$$

Considering equations which are derived for  $V_y$  and  $N_s$ , Eq. (15) for the equivalent force can be rewritten as Eq. (17).

$$F = -\frac{dV_y}{d\varphi} \cos \alpha - \frac{1}{R} \sin \alpha \times \frac{E J_z}{R^2} \left[ \frac{d^2v}{d\varphi^2} + \frac{dv}{d\varphi} \right] \quad (17)$$

As the last boundary condition it is assumed that the monofilaments are symmetrical curved bars. Therefore for the middle point of the curved bar length, we have:

$$\frac{dv}{ds} \Big|_{\varphi=0} = 0 \quad (18)$$

By the above mentioned boundary conditions, the unknown coefficients can be obtained in Eq. (9) and as a consequence, the radial deflection of the curved bar in any position along its length can be calculated. As it can be inferred the longitudinal deformation of the bar has been neglected. To apply this curved bar theory for WKSF, the exerted forces in each curved monofilament should be calculated regarding the compression load on the fabric. These forces are introduced in Eq. (15) to determine the boundary conditions needed in Eq. (9). As a result, in the following sections, three modelling approaches are utilized based on three different assumptions related to initial monofilament shapes and configurations.

#### Model A: Deflection of the curved bars in compression

In this model, the monofilaments are assumed as curved bars in weft and warp directions *Figure 4*. Monofilaments have initial curved shapes before loading and it is supposed that this curvature remains constant during compression loading.

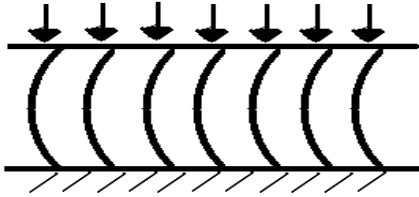


FIGURE 4. Model A: monofilaments in weft and warp directions as the curved bars in compression with an initial constant curvature radius and angle

**Model B: Deflection of the curved bar with the cantilever bar**

An initial curvature is considered for warp direction, it is supposed that this curvature remains constant during loading. The monofilaments in the weft direction are considered as a cantilever bars *Figure 5*.

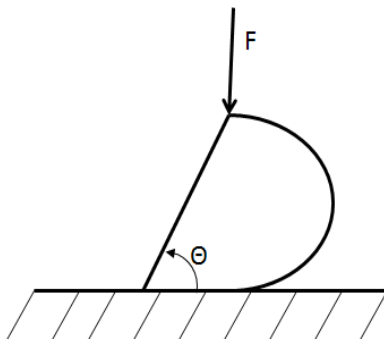


FIGURE 5. Model B: monofilaments in weft direction as cantilever bars and monofilaments in warp direction as curved bars with an initial constant curvature radius and angle

To drive the relationship between force and deflection of the fabrics as modelled in *Figure 5*, it is considered that the force on the cantilever bar is  $F_1$  and the force on the curved bar is  $F_2$ . These forces can be calculated by Eq. (19) and Eq. (20).

$$F_1 + F_2 = F \tag{19}$$

$$F_1 / K_1 = F_2 / K_2 \tag{20}$$

In which  $K_1$  and  $K_2$  are the spring constants of the cantilever and curved bar along the cantilever deflection respectively. As it is obvious, the two bars are considered to behave such as parallel springs. To

obtain  $K_2$  from the deflection theory of the bar, the deflections along normal  $\delta_1$  and axial  $\delta_2$  directions of the cantilever bar has been calculated as follow [9]:

$$\begin{cases} \delta_1 = \frac{F_1 \cos(\theta) L^2}{3EI} \\ \delta_2 = \frac{F_2 \sin(\theta) L}{EA} \end{cases} \tag{21}$$

Where  $E$  and  $I$  are the Young modulus and bending moments of the bar and  $L$  is the length of the cantilever bar. The total cantilever deflection of the cantilever bar  $\delta$  is:

$$\delta = \delta_1 \cos(\theta) + \delta_2 \sin(\theta) \tag{22}$$

The spring constant cantilever bar in the cantilever deflection can be obtained as:

$$K_1 = F_1 / \delta \tag{23}$$

By substituting Eq. (22) in Eq. (23), the spring constant of the cantilever bar  $K_1$  can be obtained. By calculating cantilever bar  $K_1$  and also using curved bar theory as presented in previous section,  $K_2$  can be determined by solving Eq. (19) and Eq. (20) together. By this way the forces on cantilever and curved bars ( $F_1$  and  $F_2$ ) will be obtained. Achieving these forces, the deflections of the bars and consequently the deflections of the fabric will be calculated as a function of the exerted forces.

**Model C: Modelling of the monofilaments with two different curved bars**

To make more realistic model to predict the compressibility behaviour of the spacer fabric, the monofilaments in both warp and weft directions have been considered as the curved bars in model C. The schematic representation of the monofilament configuration used in model C has been depicted in *Figure 6*.

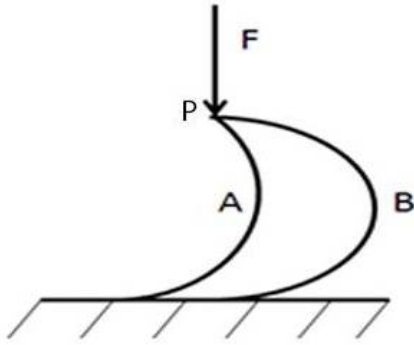


FIGURE 6. Model C: configuration of the monofilaments in WKSF: monofilament A in weft direction, monofilament B in warp direction modelled as the curved bars with variable curvature radius and angle

As it is described previously in the modelling of cantilever and curved bars, the force in each curved bars are inversely proportional to their spring constants. Additionally the spring constants of each curved bars are implicitly related to the force. To calculate the deflection due to an exerted force, the theoretical procedure similar to model A, is used here. Therefore to obtain the forces in each curved bar and also the cantilever deflections, Eq. (24) to Eq. (27) are solved simultaneously:

$$F_A = K_A \times \delta_A \quad (24)$$

$$F_B = K_B \times \delta_B \quad (25)$$

$$\frac{F_A}{K_A} = \frac{F_B}{K_B} \quad (26)$$

$$F_A + F_B = F \quad (27)$$

Where  $\delta$  is the cantilever deflection of the both curved bars.  $F_A$  and  $F_B$  are the components of force  $F$  applied on point  $P$  in weft and warp directions respectively.

To solve Eq.(24-27) simultaneously, an iterative approach is utilized as follow:

- $F_A$  is assumed.
- $F_B$  is calculated from Eq.(27).
- $K_A$ ,  $K_B$ ,  $\delta_A$  and  $\delta_B$  are calculated based on curved bar theory

If the equality in Eq.(26) is true i.e. the deflection continuity in monofilament intersection exists, the assumed values for  $F_A$  and  $F_B$  are the right values, if not, the process should return to the first step again.

It is worthy to mention that the design parameters of the fabric are present in the theoretical model implicitly. The thickness and density of the fabric are taking into account in the radius of the curved bar and the force which is exerted on each monofilaments respectively. The centre position of the monofilaments is related to angle in the way that they are connected to surface layers. The cross section radius of the monofilaments and its mechanical property is considered in  $I_z$  and  $E$  respectively.

### FABRIC CHARACTERISTICS AND TESTS

The 3-D spacer fabric configuration studied in this paper is shown in Figure 7 and 8. As it can be seen two bi-directional woven face sheets are connected with cantilever woven piles.

The monofilaments in the face sheets are in the warp direction, along which the 3-D spacer fabric is rolled up. The fabric structure design parameters can be selected and be variable depending on the fabrication process: the pile height, the distribution density of piles, the anisotropy distribution of the yarns in the warp and the weft directions etc.

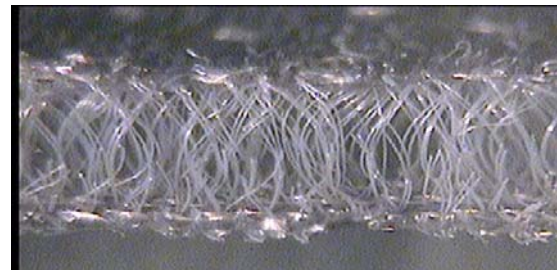


FIGURE 7. Spacer fabric in weft direction

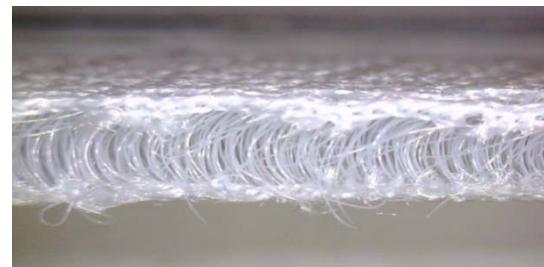


FIGURE 8. Spacer fabric in warp direction

In this work, the 3-D spacer fabric is woven with Polyester fibres, produced by Rachel warp knitting machine with two needle bars with specific thicknesses, densities and texture designs presented in *Table I* and *Table II*. The characteristics of monofilaments as Young modulus and dimensional properties used in theoretical models are given in *Table II*.

The compression tests are carried out on traction-compression machine Instron 5566. The compression loading ramp is applied with the rate of  $1 \frac{mm}{min}$  to reach a maximum pressure  $21 \frac{ib}{in^2}$ . In different compression steps, the specimen photos have been

taken in both sides to measure experimentally the variation of curvature angle and curvature radius in weft and warp directions with loading increase. This measurement of curvature variation has been utilized in theoretical model C. To measure the angle of monofilament and radius of curvature, a camera is used to capture photos from both sides of spacer fabrics during loading. A manual curve fit is used to match the monofilament curvatures, so to find the curvature angle. To determine the curvature radius, the thickness reduction is scaled using the measurement values of Instron machine and a direct dimension measurement on photos *Figure 9*. Therefore,  $\alpha$  and R are calculated for each loading step for both sides in weft and warp directions.

TABLE I. Characteristics of the spacer fabric sample (10cm×10cm).

Weight (gr)	Thickness(mm)	Linear density (Tex)	Yarn Material	Density(cpc)	Type layer	sample
5.21	8.68	7.78(34f)	Polyester	19	External upper layer	Raw Fabric (p7)
		2.23monofilament	polyester		Connectors	
		11.22(48f)	Polyester		External lower layer	

TABLE II. Characteristics of the monofilament

Density ( $\frac{gr}{cm^3}$ )	Radius of surface area (m)	Modulus (cN/Tex)	Max Stress (cN/Tex)	Extensi on at max load (%)
1.52	$2.161 \times 10E^{-5}$	52.39	3.27	7.21

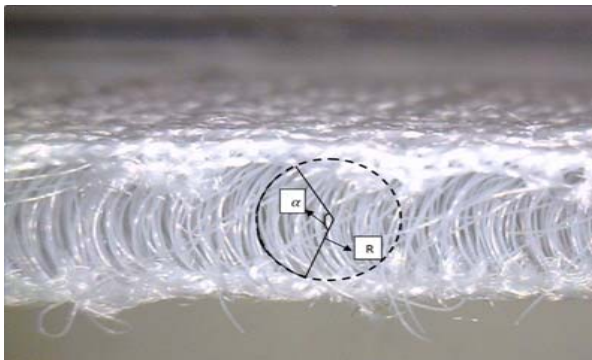


FIGURE 9. Curve fit to determine  $\alpha$  and R of monofilament.

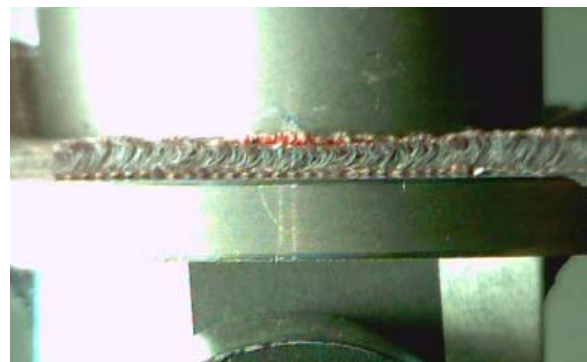


FIGURE 10. Photo of Spacer fabric under compression.

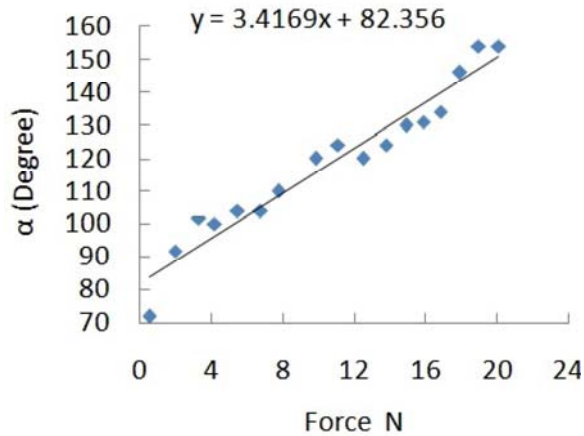


FIGURE 11. Variation of angle curvature in warp direction during compression increase.

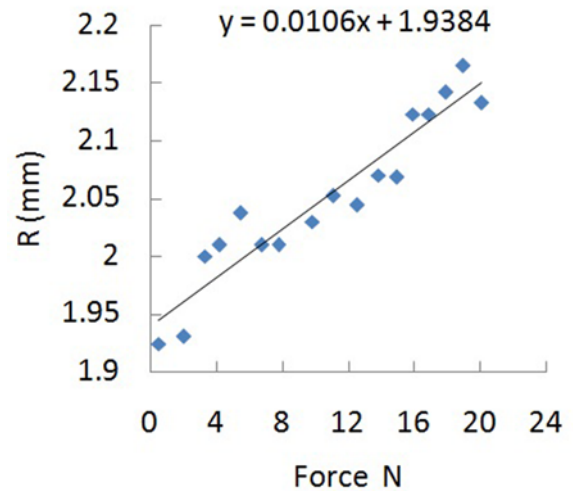


FIGURE 14. Variation of curvature radius in weft direction during compression increase.

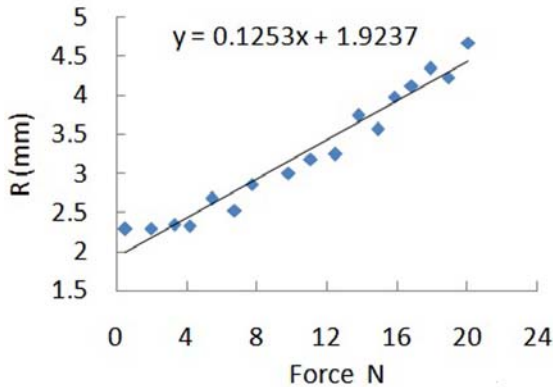


FIGURE 12. Variation of curvature radius in warp direction, during compression increase

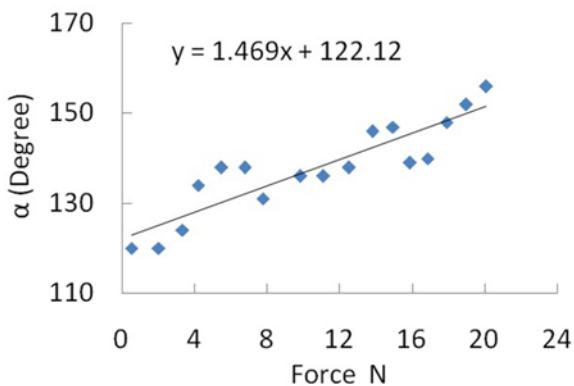


FIGURE 13. Variation of angle curvature in weft direction during compression increase.

As shown in *Figure 11, 12, 13 and 14*, the curvature radius and angles for warp and weft directions respectively increase with compression force increase as it was expected. The initial curvature radius and angles depend on the structural design of each fabric. A curve fitting is presented in order to provide an analytical expression based on experimental data for the variation of curvature radius and angle with compression loading for P7 –WKSF (Table I) as it will be useful for the fabricant industry for further investigations. So, one could find these variations for a different rang of compression loading depending on different applications.

## RESULTS AND DISCUSSION

The stress-strain curve of the spacer fabric reported in reference [3] is given in *Figure 15*. Three distinct regions in this curve can be observed: modulus, collapse and densification regions. The modulus of elasticity is defined as the initial slope in the linear elastic part of the stress-strain curve (modulus region). The initiation of collapse region is characterised by a relatively large deformation that occurs with a constant stress. During this stage, the monofilaments bend, so the thickness of the spacer fabric will decrease.

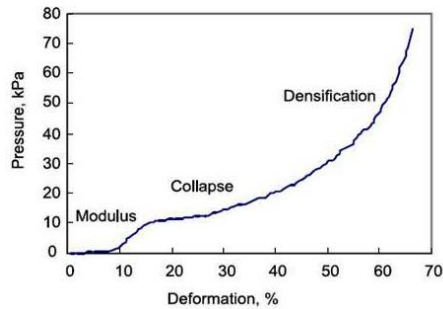


FIGURE 15 .Stress-strain curve for spacer fabric in compression[3].

This constant stress is referred to a collapse stress or a collapse plateau. The most compressibility behaviour and deformation of 3D fabrics occurs in this region, this is why this region is the subject of many investigations in the cushion fabric mechanical behaviour. In the densification region, monofilaments are engaged to each other and the deflection change decreases; the slope of stress-strain curve will decrease [3].

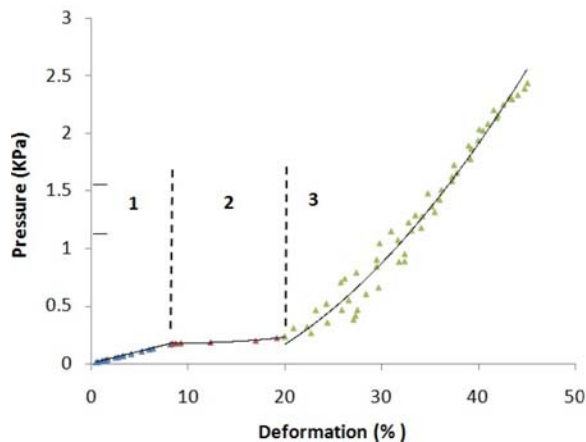


FIGURE 16. Stress-strain results obtained experimentally for tested spacer fabric in compression.

In *Figure 16*, the experimental results obtained for 3D fabric sample have been depicted. *Figure 16* shows that a typical compressibility behaviour as presented in *Figure 15* is obtained for the 3D fabric sample tested here. Modulus, collapse and densification regions are present and appear under 40% deformation. So, the maximum compression loading in experimental tests is sufficient to make appear these three regions for the studied spacer fabric here.

In *Figure 17*, the simulation results obtained by the theoretical models A, B and C are compared with experimental results for 3D spacer fabric. It can be seen that there exist a significant deviation of simulation results obtained by model A and B from experimental results whereas a good agreement between the experimental results and the simulation results obtained by model C has been observed.

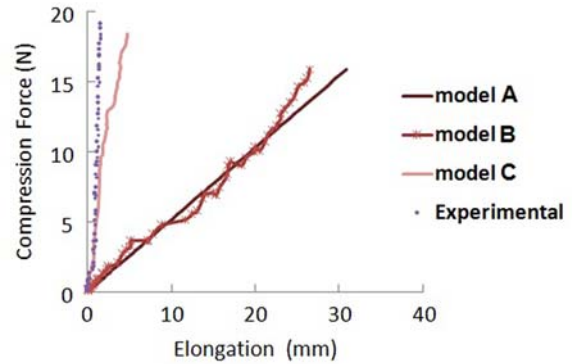


FIGURE17. Compressibility behaviour of P7-WKSF obtained by different models compared with experimental results

The deviation from experimental results in models A and B can be justified as follow. In model A, all monofilaments are considered first to have the same curvatures and second their curvature radius and angles are assumed constant during compression loading. As it can be seen by observation on tested fabrics, not only the curvature in weft direction is different from warp direction but also these curvatures change during loading process. *Figures 11, 12, 13 and 14* show that the curvature radius and angles increase with increasing compression load in experimental tests. Although model B comparing to model A has been improved by considering different initial shapes for monofilaments in weft and warp directions, but the assumption raised from considering constant curvature and angle during loading is still applied and could generate the erroneous result. In fact, the initial curvatures and angles of monofilaments in weft and warp directions change during compression loading. As a result, there is no wonder to observe that in *Figure 17*, using model B, a same order of deviation still remains between theoretical and experimental results. *Figure 18* depicts the comparison of experimental results with theoretical results obtained by model C in the modulus, collapse and densification regions.

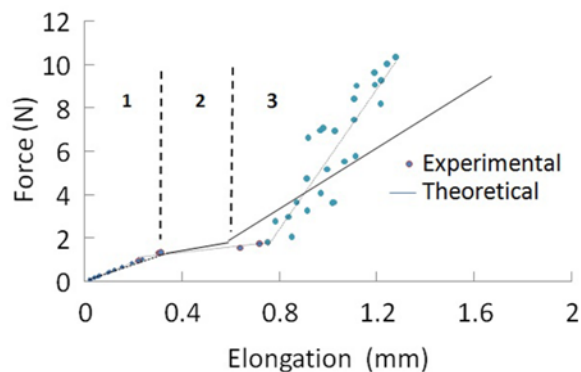


FIGURE18. Comparison of experimental results with theoretical data obtained by model (C)

As it is shown in *Figure 18*, three distinct regions can be noticed. In modulus and collapse regions, theoretical results almost agree with the experimental results. This can be explained by the fact that in this model the variations of the curvature radius and angle of the curved monofilaments in weft and warp directions have been considered conforming to the experimental observation presented in *Figure 11* up to *Figure 14*.

Also, in this region, the monofilaments have small deflections and the linear mechanical modelling used in curved bar theory could acceptably predict the force-elongation behaviour.

In densification region (region III), due to the large deflection of the monofilaments comparing to their initial length, the deviation between experimental and theoretical results increased. The simulation data obtained by model C overestimate the elongation of monofilament under compression loading. This is mainly because the curved monofilaments are compressed into each other when large deflection occurred. When the monofilaments engaged into each other in densification region, more mechanical energy dissipate during deflection, so more force is needed to generate each unit elongation of monofilaments. Moreover, the proposed model is based on the deflection of curved bars in the elastic region without considering the plastic deformation of monofilament under high compression load in densification region. So to predict the mechanical behaviour of these spacer fabrics in high loads, the model C should be modified by integration of the plastic behaviour of monofilaments. Finally, the inter effect of two layers on both sides of pile yarns should be considered. The stiffness of these layers can affect the experimental results. Therefore the slope of the

experimental results is higher than the theoretical ones.

## CONCLUSION

Three theoretical elastic models have been proposed and developed in order to predict the compressibility behaviour of monofilaments in spacer fabrics. The last modified model (model C), based on elastic curved bar theory, takes into account not only the initial curvature radius and the angle of monofilaments in weft and warp directions but also the variation of these parameters during compression. The results show that this model could better predict the elastic compressibility behaviour of spacer fabrics with similar texture design and initial curved monofilaments in weft and warp directions comparing to previous models. In modulus and collapse regions, theoretical results almost agree with the experimental ones.

## REFERENCES

- [1] Murthyguru,I, “*Novel approach to Study Compression Properties in Textile*”, *Autex Res. J.*, Vol. 5, No 4, 2005
- [2] Wensheng,H.; “*Online characterization of fabric compression behaviour*”,Phd Thesis, Fiber and Polymer, North Crolina State University,1999
- [3] Xu-hong,M.;Ming-qiao,G.;“*The Compression Behaviour of the Warp Knitted Spacer Fabric*”, *Fiber and textile in Eastern Europe*,Vol.16,No.1,pp-56-61, March 2008
- [4] Vassiliadis,S.; Kallivretaki,A; Provatidis,C.; “*Numerical modeling of the compressional behavior of warp-knitted spacer fabrics*” *Fiber and textile in Eastern Europe*,Vol.17,No.5,pp-56-61,2009
- [5] Min Li,Shaokai Wang,Zuoguang Zhang,Boming Wu“*Effect of Structure on the Mechanical Behaviors of Three-Dimensional Spacer Fabrics Composites*” Appel Compos Mater.Springer 2009.
- [6] J.Yip,S.Ng., “*study of three-dimensional spacer fabrics:Physical and mechanical properties*” *Journal of materials processing technology*.2008,pp359-364
- [7] Musiol,M.;“*Analysis of Transverse Deformation Of Spacer Products*” *AUTEX Research Journal*,Vol.5.No1,March 2005
- [8] Oden ,J.T.; “*Mechanics of Elastic Structures*”,McGraw-Hill,inc,Usa,1967,pp130-136.
- [9] Popov,E.; “*Strength of Material*”,Prentice Hall,1998

**AUTHORS' ADDRESSES**

**Fatemeh Mokhtari**

**Mahnaz Shamshirsaz**

**Masoud Latifi, Ph.D**

**Mohammad Maroufi, MSc**

Amirkabir University of Technology

(Tehran Polytechnic)

New Technologies Research Center

424 Hafez Ave.

Tehran, Tehran 15875-4413

IRAN